8-2015

Characterization of a Novel Megabirnavirus from *Sclerotinia sclerotiorum* Reveals Horizontal Gene Transfer from Single-Stranded RNA Virus to Double-Stranded RNA Virus

Minghong Wang
Huazhong Agricultural University, China

Yong Wang
Huazhong Agricultural University, China

Xiangzhong Sun
Huazhong Agricultural University, China

Jiasen Cheng
Huazhong Agricultural University, China

Yanping Fu
Huazhong Agricultural University, China

See next page for additional authors

Authors
Minghong Wang, Yong Wang, Xiangzhong Sun, Jiasen Cheng, Yanping Fu, Huiquan Liu, Daohong Jiang, Said A. Ghabrial, and Jiatao Xie

Characterization of a Novel Megabirnavirus from *Sclerotinia sclerotiorum* Reveals Horizontal Gene Transfer from Single-Stranded RNA Virus to Double-Stranded RNA Virus

Notes/Citation Information
Published in *Journal of Virology*, v. 89, no. 16, p. 8567-8579.

Digital Object Identifier (DOI)
http://dx.doi.org/10.1128/JVI.00243-15

JVI Journals.ASM.org

Characterization of a Novel Megabirnavirus from *Sclerotinia sclerotiorum* Reveals Horizontal Gene Transfer from Single-Stranded RNA Virus to Double-Stranded RNA Virus

Minghong Wang,[a,b] Yong Wang,[a] Xiangzhong Sun,[a] Jiasen Cheng,[a] Yanping Fu,[a] Huiquan Liu,[c] Daohong Jiang,[a] Said A. Ghabrial,[d] Jiatao Xie[a]

State Key Laboratory of Agricultural Microbiology, The Provincial Key Lab of Plant Pathology of Hubei Province, College of Plant Science and Technology, Huazhong Agricultural University, Wuhan, People's Republic of China[a]; College of Forestry and Horticulture, Hubei University for Nationalities, Enshi, People's Republic of China[b]; NWAFU-PU Joint Research Center, State Key Laboratory of Crop Stress Biology for Arid Areas, College of Plant Protection, Northwest A&F University, Yangling, Shanxi Province, People's Republic of China[c]; Department of Plant Pathology, University of Kentucky, Lexington, Kentucky, USA[d]

ABSTRACT

Mycoviruses have been detected in all major groups of filamentous fungi, and their study represents an important branch of virology. Here, we characterized a novel double-stranded RNA (dsRNA) mycovirus, *Sclerotinia sclerotiorum* megabirnavirus 1 (SsMBV1), in an apparently hypovirulent strain (SX466) of *Sclerotinia sclerotiorum*. Two similarly sized dsRNA segments (L1- and L2-dsRNA), the genome of SsMBV1, are packaged in rigid spherical particles purified from strain SX466. The full-length cDNA sequence of L1-dsRNA/SsMBV1 comprises two large open reading frames (ORF1 and ORF2), which encode a putative coat protein and an RNA-dependent RNA polymerase (RdRp), respectively. Phylogenetic analysis of the RdRp domain clearly indicates that SsMBV1 is related to *Rosellinia necatrix* megabirnavirus 1 (RnMBV1). L2-dsRNA/SsMBV1 comprises two nonoverlapping ORFs (ORFA and ORFB) encoding two hypothetical proteins with unknown functions. The 5′-terminal regions of L1- and L2-dsRNA/SsMBV1 share strictly conserved sequences and form stable stem-loop structures. Although L2-dsRNA/SsMBV1 is dispensable for replication, genome packaging, and pathogenicity of SsMBV1, it enhances transcript accumulation of L1-dsRNA/SsMBV1 and stability of virus-like particles (VLPs). Interestingly, a conserved papain-like protease domain similar to a multifunctional protein (p29) of *Cryphonectria* hypovirus 1 was detected in the ORFA-encoded protein of L2-dsRNA/SsMBV1. Phylogenetic analysis based on the protease domain suggests that horizontal gene transfer may have occurred from a single-stranded RNA (ssRNA) virus (hypovirus) to a dsRNA virus, SsMBV1. Our results reveal that SsMBV1 has a slight impact on the fundamental biological characteristics of its host regardless of the presence or absence of L2-dsRNA/SsMBV1.

IMPORTANCE

Mycoviruses are widespread in all major fungal groups, and they possess diverse genomes of mostly ssRNA and dsRNA and, recently, circular ssDNA. Here, we have characterized a novel dsRNA virus (*Sclerotinia sclerotiorum* megabirnavirus 1 [SsMBV1]) that was isolated from an apparently hypovirulent strain, SX466, of *Sclerotinia sclerotiorum*. Although SsMBV1 is phylogenetically related to RnMBV1, SsMBV1 is markedly distinct from other reported megabirnaviruses with two features of VLPs and conserved domains. Our results convincingly showed that SsMBV1 is viable in the absence of L2-dsRNA/SsMBV1 (a potential large satellite-like RNA or genuine genomic virus component). More interestingly, we detected a conserved papain-like protease domain that commonly exists in ssRNA viruses, including members of the families *Potyviridae* and *Hypoviridae*. Phylogenetic analysis based on the protease domain suggests that horizontal gene transfer might have occurred from an ssRNA virus to a dsRNA virus, which may provide new insights into the evolutionary history of dsRNA and ssRNA viruses.

Mycoviruses (or fungal viruses) with RNA or, rarely, DNA genomes are ubiquitous in plant-pathogenic fungi (1, 2). Based on genome nature, all known RNA mycoviruses were classified into three groups: double-stranded RNA (dsRNA), positive-sense single-stranded RNA (+ssRNA), and the recently discovered negative-sense single-stranded RNA (−ssRNA) (3, 4). Mycoviruses with dsRNA genomes are usually encapsidated in rigid particles and are so far classified into six families, including two newly established families, *Megabirnaviridae* and *Quadriviridae* (1, 5, 6). However, an increasing number of newly discovered and characterized dsRNA mycoviruses remain unassigned (7, 8).

The relationship between the presence of mycoviruses and their impact on their fungal hosts is complicated. Most of the known mycoviruses cause little or no obvious symptoms on their hosts, and a very few mycoviruses have been shown to benefit their fungal hosts (9, 10). The majority of studies have so far focused on

Received 28 January 2015 **Accepted** 1 June 2015

Accepted manuscript posted online 10 June 2015

Citation Wang M, Wang Y, Sun X, Cheng J, Fu Y, Liu H, Jiang D, Ghabrial SA, Xie J. 2015. Characterization of a novel megabirnavirus from *Sclerotinia sclerotiorum* reveals horizontal gene transfer from single-stranded RNA virus to double-stranded RNA virus. J Virol 89:8567–8579. doi:10.1128/JVI.00243-15.

Editor: A. Simon

Address correspondence to Jiatao Xie, jiataoxie@mail.hzau.edu.cn.

Supplemental material for this article may be found at http://dx.doi.org/10.1128/JVI.00243-15.

doi:10.1128/JVI.00243-15

mycoviruses that are associated with hypovirulence or other phenotypic changes in economically important phytopathogenic fungi (4). The hypovirulence-associated mycoviruses have the potential for development as biocontrol agents for combating fungal diseases and for exploitation as tools to explore the basic biology of their fungal hosts (1, 2, 11). A hypovirulent strain of *Cryphonectria* hypovirus 1 (CHV1) was successfully used for biocontrol of the chestnut blight disease in Europe (12, 13). *Sclerotinia sclerotiorum* hypovirulence-associated DNA virus 1 (SsHADV1) was successfully demonstrated to be effective in reducing *Sclerotinia* disease incidence under field conditions (14, 15). Thus, virocontrol (biocontrol of plant fungal diseases via application of mycoviruses) is a viable approach for biological control of fungal diseases under both forest and agricultural ecological systems.

The ascomycetous fungus *Sclerotinia sclerotiorum* is one of the most devastating plant pathogens, infecting more than 450 plant species (16). This phytopathogenic fungus causes stem rot disease, which is the most important disease of rapeseed and is responsible for enormous economic losses every year in China. Currently, environmentally friendly strategies, including breeding for resistance to control this disease, are unavailable. Application of chemical fungicides has some potential risks to the environment and human health and is difficult to justify due to increased public sentiment against the use of chemical fungicides. Stem rot disease, caused by the fungus *S. sclerotiorum*, represents therefore a significant economic and public relations problem. Screening for hypovirulence-related mycoviruses from populations of *S. sclerotiorum* is an initial step to virocontrol as an optional strategy for stem rot disease. Moreover, *S. sclerotiorum* is known to host various mycoviruses belonging to at least five virus families, including *Partitiviridae*, *Alphaflexiviridae*, *Hypoviridae*, *Endornaviridae*, and *Narnaviridae*, in addition to three unassigned novel mycoviruses (2, 3). Importantly, at least 10 hypovirulence-associated mycoviruses have been recently identified and demonstrated to have a promising potential as virocontrol agents for *Sclerotinia* diseases (2, 3, 17, 18). *Sclerotinia* mycoviruses show rich diversity and contribute to establishment of a new host-mycovirus system (*S. sclerotiorum*-mycovirus) for studying virus-host interactions. This interaction system will help to elucidate the molecular basis of fungal pathogenicity and interactions between mycoviruses and their host at the molecular level. Therefore, it is necessary to discover more new hypovirulence-associated mycovirus isolates for virocontrol of stem rot of rapeseed or mycovirus-related latent infection to enrich mycoviral ecology research. The newly discovered mycoviruses not only enrich virocontrol resources but also enhance research on mycoviral ecology.

In this study, we demonstrate that *S. sclerotiorum* strain SX466 harbors three unrelated mycoviruses (two with dsRNA genomes and one with an ssRNA genome) and determine the full-length cDNA sequence of a novel dsRNA virus (*Sclerotinia sclerotiorum* megabirnavirus 1 [SsMBV1]) and the genomic organization of SsMBV1. L1-dsRNA/SsMBV1 is similar to a previously reported bisegmented dsRNA mycovirus, *Rosellinia necatrix* megabirnavirus 1 (RnMBV1), whereas L2-dsRNA/SsMBV1 contains a conserved papain-like protease domain, and phylogenetic analysis suggests that horizontal gene transfer (HGT) may have occurred from an ssRNA virus (hypovirus) to a dsRNA virus (SsMBV1). Transfection experiments suggest that SsMBV1 has little or no impact on *S. sclerotiorum*.

MATERIALS AND METHODS

Fungal strains and culturing. Strain SX466 was isolated from a sclerotium collected from a diseased stem of rapeseed plant (*Brassica napus*) in Shanxi Province, People's Republic of China. *S. sclerotiorum* virus-free strain Ep-1PNA367 was a single-ascospore isolate of strain Ep-1PN (19) and served as a recipient strain for virus-like particle (VLP) transfection assays. *S. sclerotiorum* strain 1980 is a reference strain whose genome has been sequenced (20). Strain 1980R was genetically labeled with a hygromycin resistance gene and served as a recipient strain for horizontal transmission assays. To further confirm that strain SX466 is an isolate of *S. sclerotiorum*, the ribosomal DNA (rDNA) gene fragment of the internal transcript spacer (ITS) of strain SX466 was amplified and sequenced. The results showed that SX466 is unquestionably an isolate of *S. sclerotiorum*. All *S. sclerotiorum* strains and their derivatives in this study were maintained at 20°C on potato dextrose agar (PDA) and stored at 4°C on PDA slants, and the dried sclerotia were stored at −20°C.

Extraction of VLPs and electron microscopy observations. Virus-like particles (VLPs) were isolated from mycelia of strain SX466 via differential centrifugation and concentrated by sucrose density gradient centrifugation as previously described with minor modifications (5, 21). The VLPs were suspended in 100 μl of 0.05 M sodium phosphate buffer (pH 7.4) and then used for SDS-PAGE, polypeptide mass fingerprint-mass spectrum (PMF-MS) analyses, transmission electron microscope (TEM) observations, dsRNA extraction, and infectivity assays.

Extraction and purification of dsRNA from mycelium and VLPs. *S. sclerotiorum* strains for dsRNA extraction were cultured on PDA overlaid with a cellophane membrane for 4 days, and mycelium was collected with a sterile spatula. dsRNA was extracted from fungal mycelia by CF-11 cellulose (Sigma-Aldrich, Dorset, England) chromatography, whereas the dsRNA from purified VLPs was released by using phenol-chloroform extraction as described previously (22). Samples of dsRNA were successively treated with DNase I and S1 nuclease (TaKaRa, Dalian, China) and separated by agarose gel electrophoresis. The dsRNA bands were cut from an ethidium bromide-containing agarose gel with a sterile knife under UV illumination and then were purified with a gel extraction kit (Axygene, Hangzhou, China). The purified dsRNA was stored at −20°C or used for cDNA cloning or Northern blot analysis.

Full-length cDNA cloning and sequencing. To characterize the dsRNA segments, cDNA libraries were constructed according to previous reports (23), using a cDNA synthesis kit (Fermentas, Ontario, Canada) with a tagged random primer, dN6 (5′-CGATCGATCATGATGCAATG CNNNNNN-3′). Briefly, the purified dsRNA (about 100 ng) was denatured with 10% dimethyl sulfoxide (DMSO) at 98°C for 15 min and then reverse transcribed according to the manufacturer's instructions. The reverse transcription (RT) products were treated with NaOH (0.1 M final concentration at 68°C for 60 min) for denaturation, and then HCl and Tris-HCl (pH 8.0) with 0.1 M final concentrations were used for neutralization and annealing. The reaction contents were incubated at 68°C for 1 to 2 h, and a mixture of partial double-stranded cDNAs (dscDNAs) was synthesized. *Taq* DNA polymerase was used for synthesis of complete dscDNAs. The random dscDNA products were then amplified from the constructed dscDNA library using a single specific primer (5′-CGATCG ATCATGATGCAATGC-3′) and were ligated into pMD18-T vector (TaKaRa, Dalian, China) according to the manufacturer's recommendations. Recombinant colonies were randomly selected, and individual clones containing dscDNA inserts (>0.5 kb) were identified by nucleotide sequence analysis. Gaps in the sequence were filled in by RT-PCR with sequence-specific primers designed according to sequences flanking the gaps.

The 5′- and 3′-terminal sequences were determined by RACE-PCR (rapid amplification of cDNA ends-PCR) according to a previously reported method (24). An "anchor primer," the PC3-T7 loop (5′-p-GGAT CCCGGGAATTCGGTAATACGACTCACTATATTTTTATAGT GAGTCGTATTA-OH-3′), was ligated to purified dsRNA using T4 RNA ligase and used for the RT reaction. The primer PC2 (5′-CCGAATTCCC

GGGATCC-3′), designed based on the corresponding sequence of the PC3-T7 loop, and sequence-specific primers designed based on the available sequence and proximal region sequences were used for the amplification of terminal sequences. The expected PCR products were recovered and purified with a gel extraction kit (Axygen) and then cloned into the pMD18-T vector (TaKaRa) for sequencing. To achieve high-quality consensus sequences and to avoid laboratory PCR artifacts, each nucleotide of full-length cDNA was sequenced a minimum of three times.

Sequence analysis, alignment, and phylogenetic analysis. The basic features (lengths, G+C content, etc.) of a full-length cDNA sequence of mycovirus genomic RNAs were analyzed using DNAMAN software. Potential open reading frames (ORFs) and conserved domain(s) of full-length cDNA sequence of a mycovirus were identified using the ORF finder and CD-search on the website of the National Center for Biotechnology Information (NCBI) (http://www.ncbi.nlm.nih.gov/) and the motif scan website (http://www.genome.jp/tools/motif/). All sequences of mycoviruses used in this study were retrieved from the NCBI GenBank database (http://www.ncbi.nlm.nih.gov/genomes) and used for comparative analyses. Multiple alignments of conserved sequences of RNA-dependent RNA polymerase (RdRp) or peptidase were conducted using the CLUSTAL-X program (25). Phylogenetic trees were generated using the neighbor-joining (NJ) method with 1,000 bootstrap replicates in the software of MEGA5 and SplitsTree (26, 27). The stem-loop structures of terminal sequences of mycoviruses were predicted using the program RNA folding with the default settings at the Mfold website (http://mfold.rna.albany.edu/?q=mfold/RNA-Folding-Form) (28). Prediction of RNA pseudoknots was performed using the program DotKnot (29) as implemented at http://dotknot.csse.uwa.edu.au/. The free energy value for each predicted structure was provided by the respective prediction program. The Phyre2 server was used to predict the three-dimensional structure of protein sequences with a homology modeling method (30). The structural images of proteins were created using the PyMOL molecular viewer.

Horizontal transmission assay. To explore horizontal transmission of dsRNA segments via hyphal anastomosis, strain SX466 (donor) and mycovirus-free virulent strain 1980R (recipient) were cocultured on the same PDA plates. Two mycelial agar discs from selected strains were dually cultured on a PDA plate. When the two colonies contacted each other for 48 to 72 h, mycelial agar discs were taken from the side of the recipient strain farthest from the contact point between the two colonies. All new isolates were purified by hyphal-tip isolation and cultured on PDA containing 30 μg/ml hygromycin. This process was repeated a minimum of three times. The newly virus-infected isolates were then cultured on PDA without hygromycin and tested for mycovirus content and biological properties.

Transfection of protoplasts with VLPs. Protoplast preparation of virus-free *S. sclerotiorum* strain Ep-1PNA367 was performed according to a previously described method (31). Purified VLPs (5 μl; about 50 to 200 ng) were introduced into protoplasts (about 10^6/ml) using polyethylene glycol 4000 (PEG 4000) as previously described (21). Transfected protoplasts were individually transferred to new PDA plates and incubated at 20°C until regenerated mycelia covered the surface of PDA plates. Fifteen regenerated isolates were randomly transferred to fresh cellophane-overlaid PDA to assay for mycovirus infection using dsRNA extraction and RT-PCR. All transfected regenerated isolates were subcultured at least three times to confirm mycovirus stability in each isolate.

Total RNA extraction, RT-PCR, real-time quantitative PCR, and Northern blot hybridization analysis. Total RNA from fungal strains was prepared with the TRIzol reagent (Invitrogen) and used for RT-PCR amplification to test for mycovirus content using virus-specific primers. The specific primers S1-F (5′-GTGCACCGAGCCCAACTATTGG-3′) and S1-R (5′-ACTAAACAGCTCAGGCGATTGC-3′) were used for L1-dsRNA/SsMBV1, and primers S2-F (5′-TGCCGCAACAGCTGCATTGTC-3′) and S2-R (5′-TGTGCTCCATAACACTCCACCATCA-3′) were used for L2-dsRNA/SsMBV1. Specific primers P-F (5′-GGAGGATGTGGTAG TAAAAAAGGTG-3′) and P-R (5′-ATAACGAATCTGGTAAGAACCGA GT-3′) were used for an uncharacterized partitivirus isolated from strain SX466. Two specific primers, mito-F (5′-AAATTAGGCATTGGTCTGA TCGGAT-3′) and mito-R (5′-TCCCTCAAGTCTTCGCTGCCTATAA-3′), were used for a mitovirus in strain SX466. At the same time, β-tubulin gene-specific primers SS-β-tubulin F (5′-TTGGATTTGCTCCTTTGAC CAG-3′) and SS-β-tubulin R (5′-AGCGGCCATCATGTTCTTAGG-3′) were used as an internal control.

To evaluate L1-dsRNA/SsMBV1 transcript levels in *S. sclerotiorum* in the presence or absence of L2-dsRNA/SsMBV1, relative quantification was performed with the SYBR green RT-PCR on a CFX96 real-time system (Bio-Rad, Hercules, CA, USA). Total cDNA abundance in the samples was normalized using the tubulin gene as an internal control, which was amplified by primer pair SS-β-tubulin-F–SS-β-tubulin-R.

Northern hybridization analysis was performed as previously described (22). SsMBV1 cDNA clones were labeled with digoxigenin and used to probe the RNA blot.

Growth rate and virulence assays. Mycelial growth rate, colony morphology, and results of the virulence test on detached leaves of rapeseed (*Brassica napus*) or soybean (*Glycine max*) were evaluated according to the procedures described by Zhang et al. (31). Biological property data were analyzed by one-way analysis of variance using the SAS8.0 program. Differences with P values of <0.01 were considered statistically significant.

Nucleotide sequence accession numbers. The complete nucleotide sequences of bisegmented dsRNA virus SsMBV1 reported here have been deposited with the EMBL/GenBank/DDBJ databases under accession numbers KP686398 and KP686399.

RESULTS

***S. sclerotiorum* strain SX466 carrying dsRNA segments showed hypovirulence traits.** More than 1,000 sclerotia were isolated from diseased rapeseed plants in Shanxi Province, China. All the sclerotia were repurified using conventional methods under laboratory conditions and then screened for abnormal colony morphology on PDA plates kept at 20°C. One among more than 50 isolates with abnormal colony morphology, designated strain SX466, was further characterized in the present study.

Although strain SX466 was originally isolated from a sclerotium, this strain lost its capability to produce sclerotia and its phenotype was markedly different from that of normal *S. sclerotiorum* isolates. Compared to virus-free strain Ep-1PNA367, strain SX466 showed abnormal colony morphology and lower growth rate (1.3 cm/day compared to 2.3 cm/day for virus-free strain Ep-1PNA367) (Fig. 1A and B, respectively). The virulence assays of these two strains were performed on detached rapeseed leaves. Strain SX466 formed a small lesion with a diameter of 0.8 cm, whereas strain Ep-1PNA367 caused a larger and a typical disease lesion on leaves with a diameter of 2.7 cm (Fig. 1C and D). Thus, SX466 is an *S. sclerotiorum* strain with abnormal colony morphology and is relatively less virulent than the virus-free strain Ep-1PNA367.

As strains with abnormal phenotypes usually carry mycoviruses based on previous reports, dsRNA segments were extracted from mycelia of strain SX466 and separated on 1% agarose gels. Following digestion of the dsRNA samples with DNase I and S1 nuclease, at least four distinct dsRNA segments were visible on agarose gels under UV light and tentatively named L1-, L2-, M-, and S-dsRNAs. All dsRNA segments were purified and used for cDNA cloning.

Partial sequences of four dsRNA segments were obtained via random PCR amplification and analyzed on the NCBI website with the blastx program. The cDNA sequences of L1- and L2-dsRNA share similarity to those of *Rosellinia necatrix* megabirna-

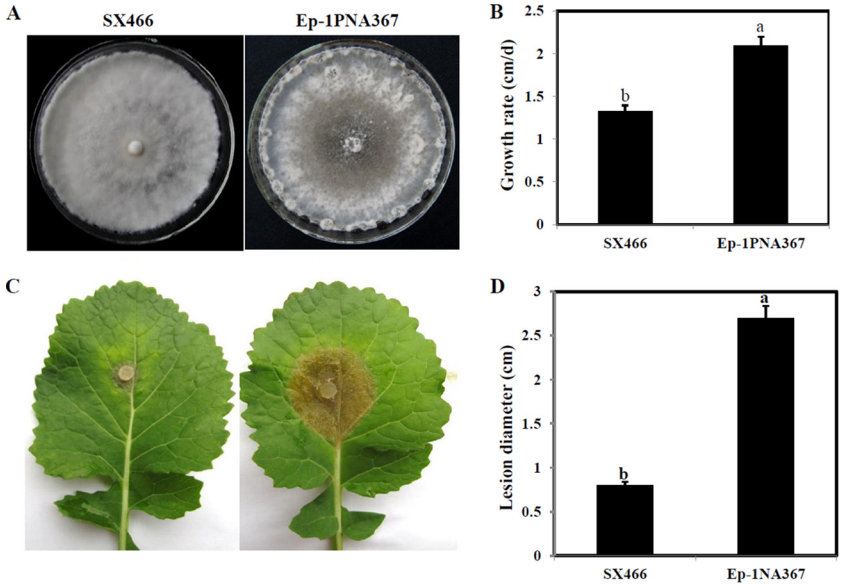

FIG 1 Biological properties of *S. sclerotiorum* strain SX466 and virus-free strain Ep-1PNA367. (A) Colony morphology. (B) Growth rate. (C and D) Virulence assay on detached rapeseed leaves. The bars represent standard deviations from the means. The lowercase letters on top of the bars indicate that the differences are statistically significant ($P < 0.01$).

virus 1 (RnMBV1). The full-length cDNA sequences of these two dsRNAs were determined in this study. M-dsRNA showed the highest sequence identity (93%) to the putative RNA-dependent RNA polymerase (RdRp) of *Sclerotinia sclerotiorum* mitovirus 2 (SsMV2) (family *Narnaviridae*) (accession number AGC24231), and thus, the M-dsRNA was presumed to represent the genome of a strain of SsMV2 based on ICTV species demarcation criteria in the genus *Mitovirus* (32). Partial cDNA sequences of S-dsRNA segments exhibited 30 to 40% amino acid sequence identity to RdRp and coat protein (CP) of *Sclerotinia sclerotiorum* partitivirus S (family *Partitiviridae*) (accession number YP_003082248), and thus, the S-dsRNA was presumed to represent a new partitivirus with a genome of two similarly sized dsRNA segments.

Purified VLPs containing L1- and L2-dsRNA segments. VLPs were isolated and purified from mycelium of strain SX466 using a 10 to 40% sucrose gradient centrifugation. VLP fractions containing dsRNA were identified by RT-PCR with specific primers designed based on cDNA sequences of dsRNA segments. For L1- and L2-dsRNA-containing fractions, rigid spherical VLPs of approximately 45 nm in diameter were observed under a TEM (Fig. 2A). Following dissociation of the purified VLPs, two clear dsRNA segments were detected in agarose gels and their migration rates were

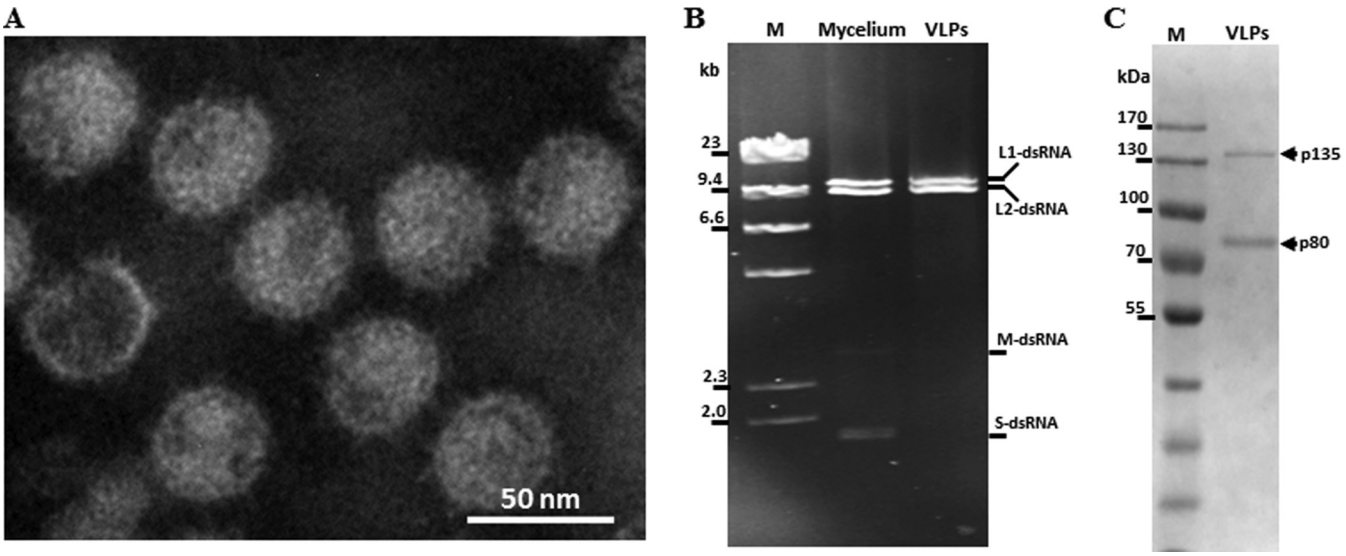

FIG 2 VLPs and dsRNA segments isolated from strain SX466. (A) VLP morphology observed under transmission electron microscopy. (B) Agarose gel electrophoresis on 1% agarose of dsRNA extracted from mycelia and purified VLPs, respectively; samples from mycelium were treated with DNase I and S1 nuclease prior to electrophoresis. Lane M, DNA molecular size markers. (C) SDS-PAGE of purified SsMBV1 VLPs (from strain SX466) on a 10% polyacrylamide gel showing two prominent bands (p135 and p80, respectively).

similar to those extracted directly from mycelium of strain SX466 (Fig. 2B). Thus, L1- and L2-dsRNA segments were presumed to be mycoviral genomes.

Protein components of SsMBV1 VLPs were separated on a polyacrylamide gel by SDS-PAGE, and two major proteins (p135 and p80) were detected with approximate sizes of 135 kDa and 80 kDa (Fig. 2C). We attempted unsuccessfully to purify partitivirus particles.

Full-length cDNA sequences, genome organization of L1-dsRNA/SsMBV1 segment, and phylogenetic analysis. To clarify the genomic organization of SsMBV1, full-length cDNA sequences of two L-dsRNA segments were determined by assembling more than 100 overlapping clones. Genome organization is depicted in Fig. 3A.

L1-dsRNA is 8,806 nucleotides (nt) in length with a GC content of 49.1% and has two large open reading frames (ORFs), ORF1 and ORF2, in different frames on the genomic plus strand. ORF1 begins with AUG at positions 1553 to 1555 and terminates with UAA at positions 5306 to 5308, and ORF2 begins with AUG at positions 5419 to 5421 and terminates with UAG at positions 8770 to 8772. The L1-dsRNA has a long 5′ untranslated region (UTR) of 1,552 nt but a relatively short 3′ UTR of 37 nt. The deduced amino acid sequence of ORF1 was found to code for a protein of 1,250 amino acid (aa) residues with a calculated molecular mass of 137 kDa, whereas ORF2 encodes a 1,116-amino-acid (aa) protein of 125 kDa. The pI values of the 137-kDa and 125-kDa proteins are 6.63 and 6.40, respectively. A BLASTP search and a conserved motif search were made using the putative protein sequences encoded by ORF1 or ORF2. The results showed that the ORF1-encoded putative protein has no sequence similarity to any known protein with the exception of coat protein (accession number YP_003288762) encoded by RnMBV1 and the ORF2-encoded protein with an RdRp domain (RdRP_4, pfam02123) and 44% identity to RdRp encoded by RnMBV1.

Although the sequences of ORF1 and ORF2 are nonoverlapping, it is notable that there are no in-frame stop codons upstream of the ORF2 start codon until the UGA at nucleotide (nt) positions 5293 to 5295 that is located upstream of the ORF1 stop codon (nt positions 5306 to 5308). RdRp appears to be expressed as a CP-RdRp fusion as evinced by the presence on the plus strand of L1-dsRNA of two *cis*-acting elements, a heptanucleotide frameshift site and a downstream pseudoknot that are required for −1 translational frameshift (33). The putative shifty heptamer motif (5299-AAAAAAC-5305) that is located upstream of the ORF1 stop codon is consistent with typical shifty heptamer motifs of "XXXYYYZ," where XXX can be any 3 identical nucleotides, YYY can be either AAA or UUU, and Z is usually not G (34). This motif could facilitate ribosomal frameshifting. The RNA pseudoknot (nt 5337 to 5403) with the ΔG value of −27.19 kcal/mol is located downstream of the shifty heptamer motif (Fig. 3B). The pseudoknot structure usually facilitates pausing of the translating ribosome and increasing the frequency of frameshifting (35). Moreover, the pseudoknot structure commonly exists in dsRNA mycoviruses belonging to the family *Totiviridae* (36). Thus, L-dsRNA probably represents a novel dsRNA mycovirus and was tentatively named SsMBV1 (*Sclerotinia sclerotiorum* megabirnavirus 1).

The potential secondary structures of 5′- and 3′-terminal sequences were predicted on the plus strand of L1-dsRNA/SsMBV1 using the Mfold program. The results showed that the 5′-terminal sequences (nt positions 1 to 55) and 3′-terminal sequences (nt positions 8755 to 8806) could be folded into potential stable stem-loop structures with ΔG values of −20.70 kcal/mol and −10 kcal/mol, respectively (Fig. 3C and D).

To better understand the relationship between SsMBV1 and other viruses, multiple alignment was performed and phylogenetic trees were constructed based on the conserved RdRp domain. Multiple alignment revealed that the RdRp domain of SsMBV1 contained eight conserved motifs (Fig. 4A). Phylogenetic analysis of the RdRp domains revealed that SsMBV1 is clustered together with RnMBV1 and thus belongs to a recently established family, *Megabirnaviridae*, with potentially the following probable members: *Phlebiopsis gigantea* large virus 1 (PgLV-1), *Lentinula edodes* mycovirus (LeMV)-HKA and LeMV-HKB, and *Lentinula edodes* spherical virus (LeSV). Members and probable members of *Megabirnaviridae* formed a clade as an independent subgroup, which is distantly related to members of the established families *Chrysoviridae*, *Totiviridae*, and *Quadriviridae* (Fig. 4B). A phylogenetic tree based on coat protein was constructed, and the result was similar to those of RdRp analysis (Fig. 4C).

Characterizations of two L2-dsRNA/SsMBV1-encoded putative hypothetical proteins containing a conserved protease domain. The full-length cDNA sequence of L2-dsRNA was determined and was deposited in GenBank. Sequence analysis indicated that it is 7,909 nt in length with a G+C content of 50.2%. Two large putative ORFs, ORFA (nt positions 1586 to 6464) and ORFB (nt positions 6521 to 7595), were identified on the positive strand of the L2-dsRNA with the 5′ UTR being 1,585 nt and the 3′ UTR being 414 nt (Fig. 3A). ORFA and ORFB were separated by 57 nt. It is important to note that the 5′ UTR sequences of L1- and L2-dsRNA share 98% sequence identity based on alignment analysis. Moreover, the first 250 nt of the 5′ UTR from the two L-dsRNAs are strictly conserved sequences and show 100% sequence identity (data not shown). Although the 5′ UTRs showed highly conserved sequences, the 3′ UTRs (32 nt) were apparently less conserved, with 43.8% (14/32) sequence identity. No other region of sequence identity between the L1- and L2-dsRNA was detected at the nucleotide and amino acid levels. The 5′-terminal sequences (nt positions 1 to 55) of L2-dsRNA formed a putative stem-loop structure that was the same as L1-dsRNA (Fig. 3C), whereas the 3′-terminal sequences (nt positions 7836 to 7909) of L2-dsRNA could be folded into a triple stem-loop structure with the ΔG value of −26.70 kcal/mol (Fig. 3E).

ORFA encoded a large putative hypothetical protein of 1,626 aa with a calculated molecular mass of 179 kDa and a predicted pI value of 6.53. A BLASTP and conserved motif search revealed that the N-terminal region (aa positions 215 to 306) of putative ORFA encoded a protein containing a conserved protease domain (Peptidase_C7, pfam01830) that has 29% sequence identity (E value = 3e−07) with papain-like cysteine protease p29 of *Cryphonectria* hypovirus 1 (CHV1), and the C-terminal region (aa positions 1016 to 1626) of ORFA-encoded protein has 33% sequence identity (E value = 5e−64) to the corresponding sequence of ORF3-encoded protein from RnMBV1 (Fig. 3A).

The three-dimensional structure of the protease domain encoded by ORFA of L2-dsRNA was predicted with Phyre2 using the principles and techniques of homology modeling (30). The helper component protease (HC-Pro) (Protein Data Bank code c3rnvA), which is a multifunctional protein, including protease activity, and is commonly encoded by viruses of family *Potyviridae* (37),

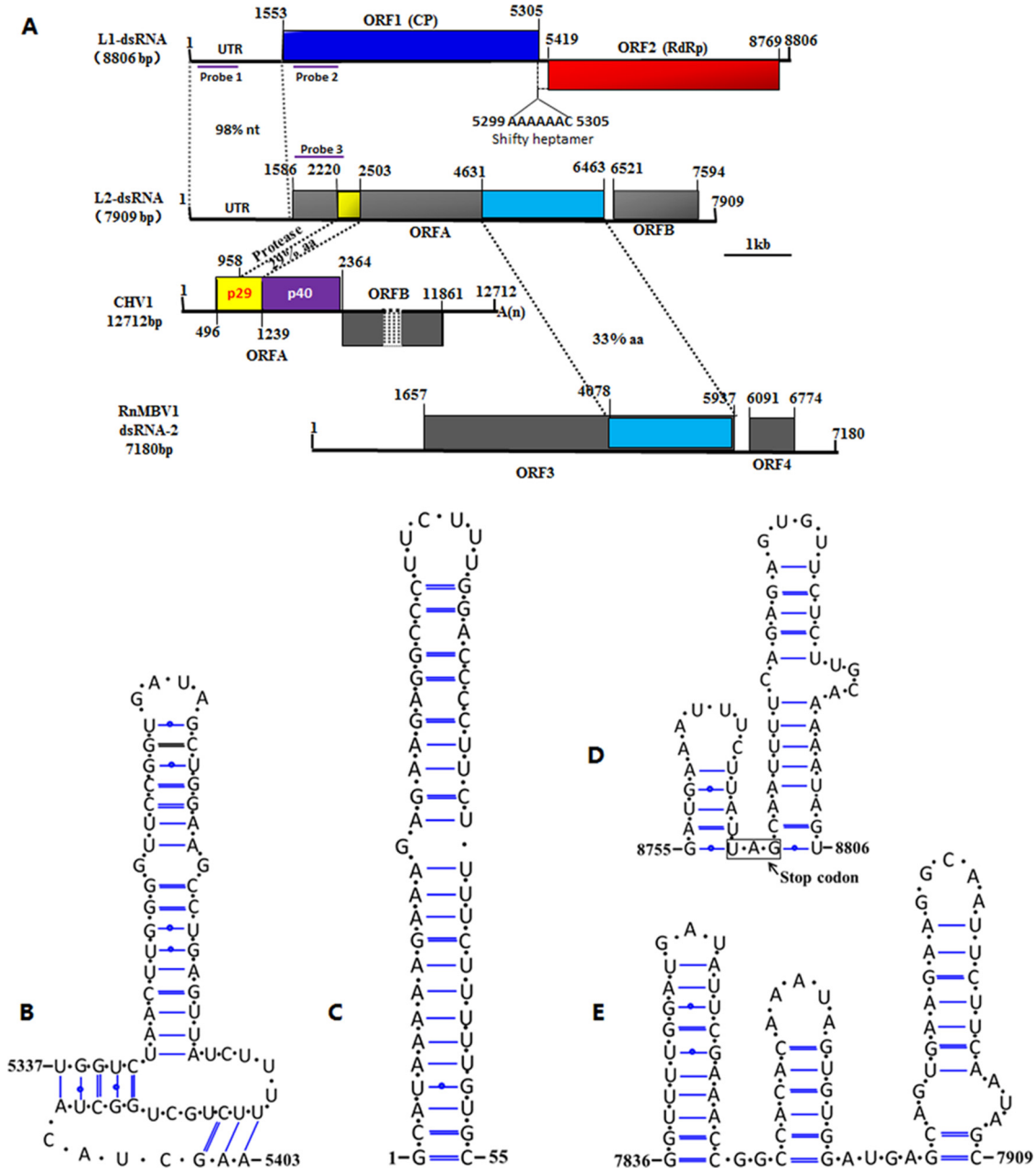

FIG 3 Molecular characteristics of L1- and L2-dsRNA segments from *S. sclerotiorum* strain SX466. (A) Schematic representation of the genomic organization of L1- and L2-dsRNAs. L1-dsRNA shows the presence of two ORFs (ORF1 and ORF2). The dotted-line box indicates a possible extension of ORF2 via a −1 translational frameshift mechanism. The putative coat protein (CP) and RNA-dependent RNA polymerase (RdRp) are shown as blue and red boxes, respectively. L2-dsRNA contains two ORFs (ORFA and ORFB) and encodes two putative hypothetical proteins with unknown functions. The ORFA-encoded protein contains a conserved domain of papain-like cysteine protease that shares 29% amino acid sequence identity with p29 of hypovirus CHV1. The C-terminal portion of the ORFA-encoded protein shares 33% amino acid sequence identity with the corresponding sequence of dsRNA2 of RnMBV1. The 5′ untranslated region (UTR) is conserved between L1- and L2-dsRNAs with 98% identity. Regions used for probes in Northern blotting (Fig. 7) are indicated by purple lines: probe 1 (nt 25 to 782) and probe 2 (nt 1587 to 2308) on L1-dsRNA and probe 3 (nt 1633 to 2250) on L2-dsRNA. (B) Predicted pseudoknot structure immediately downstream of a putative frameshift site. The RNA secondary structure was predicted by the KnotSeeker program. (C to E) Predicted secondary structures of the terminal sequences of the positive strand of L1- and L2-dsRNA. The 5′-terminal sequence of the positive strand of L1- and L2-dsRNAs could be folded into a potential stable stem-loop structure (C). Predicted secondary structures of the 3′-terminal sequences of L1- and L2-dsRNA are shown with double (D) and triple (E) stem-loop structures, respectively. Default settings were utilized for secondary structure analyses. All secondary structures are depicted in a style modified from the ones provided by the program.

was selected as the template to construct the model of the putative protease protein of L2-dsRNA. The results revealed that 87 residues were modeled with 97.2% confidence and 95% coverage of HC-Pro (Fig. 5A). The three-dimensional structure of the protease domain of L2-dsRNA was similar to that of the potyvirus 2 helper-component protease (Fig. 5B).

Bioinformatic analysis of the putative protease domain derived from ORFA-encoded protein showed that it was similar to that

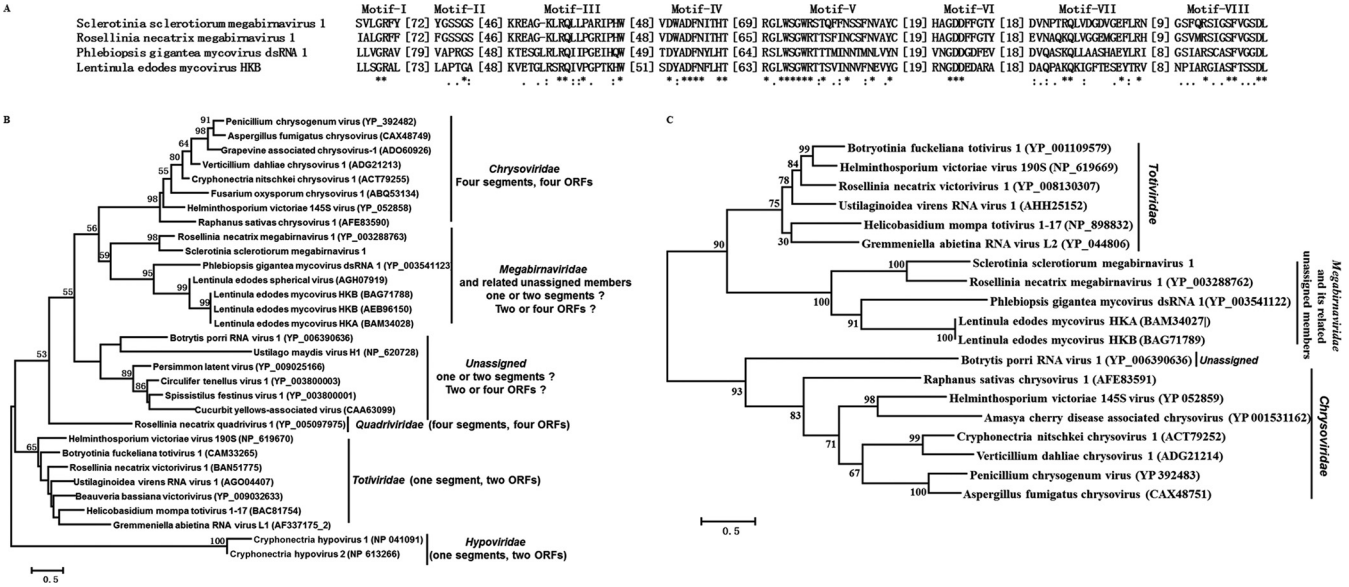

FIG 4 Multiple alignment and phylogenetic analysis of the conserved RdRp region encoded by ORF2 of L1-dsRNA/SsMBV1. (A) Multiple alignment of conserved RdRp amino acid motifs of SsMBV1 and corresponding regions in three other viruses. Eight motifs (I to VIII) are detected in the sequence of the conserved RdRp region. Identical residues are indicated by asterisks; conserved and semiconserved amino acid residues are indicated by colons and dots, respectively. Numbers in square brackets correspond to the numbers of amino acid residues separating the motifs. (B) An unrooted phylogenetic tree constructed based on an alignment of respective RdRp amino acid sequences of selected viruses. (C) Neighbor-joining unrooted phylogenetic tree constructed based on an alignment of the full-length coat protein sequences of SsMBV1, RnMBV1, and related unassigned members of family *Megabirnaviridae* using MEGA version 6.0 program. Selected viruses in families *Totiviridae* and *Chrysoviridae* were also included in the phylogenetic tree; accession numbers follow virus names. Bootstrap values (percent) obtained with 1,000 replicates are indicated on branches, and branch lengths correspond to genetic distance; the scale bar at lower left corresponds to a genetic distance of 0.5.

found in all known hypoviruses of the family *Hypoviridae*. Based on sequence alignment with eight reported hypoviruses, we found a highly conserved predicted autoproteolytic catalytic site (aa positions Cys^{222} and His^{252}), the typical characteristic of a papain-like cysteine protease, in the N-terminal region of ORFA-encoded protein. Moreover, a putative polyprotein cleavage site (aa position Gly^{306}) was detected downstream of this deduced papain-like protease domain (Fig. 6A). Phylogenetic analysis further supported that the protease domain in ORFA was most closely related to that in CHV1-ORFA and clustered in a phylogenetic clade with two other hypoviruses, CHV3 and *Fusarium graminearum* virus 1 (FgV1)-ORF1 (Fig. 6B and C). Interestingly, this clade is separated from other known hypoviruses. Hence, the protease domain of L2-dsRNA appears to be the result of horizontal gene transfer events between two ostensibly unrelated virus groups (dsRNA and ssRNA virus groups).

ORFB encoded a small putative hypothetical protein of 358 amino acids with a calculated molecular mass of 40 kDa and a predicted pI value of 8.84. There are no sequence similarities to any known proteins in the NCBI protein database. Furthermore, no conserved motifs related to replicase were observed using the PROSITE motif database and conserved domain database, suggesting that the L2-dsRNA could not replicate independently.

L2-dsRNA/SsMBV1 is dispensable for SsMBV1 replication and packaging. To further explore whether SsMBV1 is associated with phenotypic alterations in host fungal strain SX466, purified SsMBV1 VLP fractions were transfected into protoplasts of virus-free strain Ep-1PNA367 via a PEG-mediated protocol. Mycelial agar discs were taken randomly from the colonies generated from protoplasts transfected by VLPs and transferred into fresh PDA plates for subculturing for a minimum of two times. Fifteen colonies generated from protoplasts were randomly selected and individually cultured and tested for the presence of dsRNA segments. The results indicated that the purified VLPs successfully transfected protoplasts of strain Ep-1PNA367. It is interesting that all tested transfection derivatives were divided into two different types based on dsRNA content. Two-thirds of derivatives from the transfected protoplasts were found to harbor only L1-dsRNA/SsMBV1 but with loss of L2-dsRNA/SsMBV1 (such as A367V4), whereas the remaining one-third of derivatives was found to harbor both L1- and L2-dsRNA/SsMBV1 (such as isolate A367V2). These results were further confirmed by RT-PCR amplification and Northern blot analysis (Fig. 7). None of the regenerated transfectants contained L2-dsRNA/SsMBV1 alone. Since all tested transfectants were subcultured for more than 10 times via hyphal tip or protoplast isolation, L1-dsRNA/SsMBV1 is competent for replication in all tested strains of *S. sclerotiorum* regardless of whether L2-dsRNA/SsMBV1 exists. Moreover, new transfectants containing L1-dsRNA/SsMBV1 but lacking L2-dsRNA/SsMBV1 were successfully and stably transmitted to virus-free strain Ep-1PNA367 via hyphal fusion. However, compared to L2-dsRNA-free transfectants (A367V3 and A367V4), the transcript level of L1-dsRNA/SsMBV1 was markedly increased in L2-dsRNA/SsMBV1-infected transfectants (A367V1 and A367V2) (Fig. 7E).

To further explore whether L1-dsRNA/SsMBV1 alone is packaged in VLPs in the new transfectants, VLPs were reisolated from the transfectant A367V3 or A367V4, respectively. The results showed that VLPs, similar to the original VLPs extracted from strain SX466 in morphology, were observed in both new transfectants, suggesting that L1-dsRNA/SsMBV1 alone could be pack-

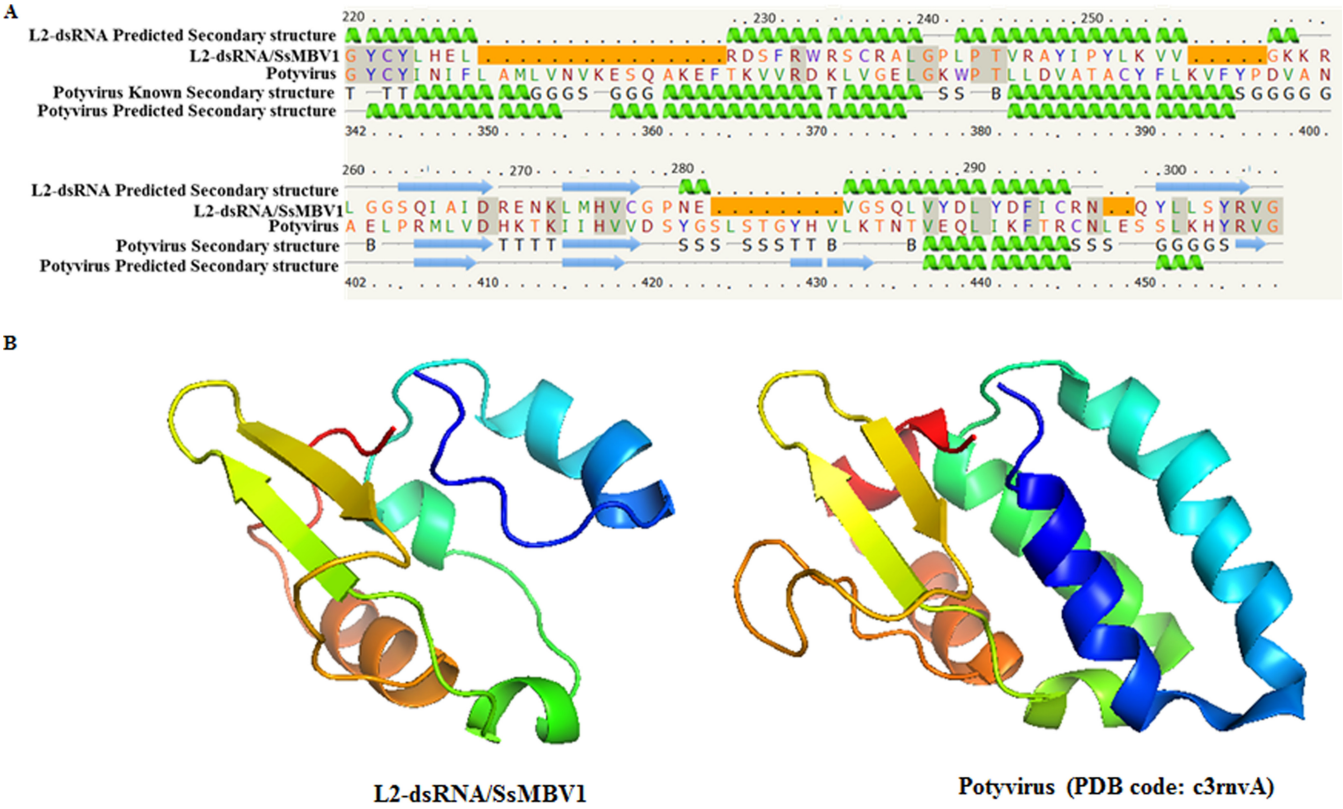

FIG 5 Prediction of a papain-like cysteine protease domain in the sequence of L2-dsRNA/SsMBV1. (A) Sequence alignment of the papain-like cysteine protease domain from L2-dsRNA/SsMBV1 and potyvirus 2 helper-component protease (Protein Data Bank code c3rnvA). Identical residues are highlighted with a gray background. Green helices represent α-helices, blue arrows indicate β-strands, and light gray lines indicate coil. G, T, B, and S in the "potyvirus known secondary structure" section represent 3-turn helix (3_{10} helix), hydrogen-bonded turn, residue in isolated β-bridge, and bend, respectively. The orange frame in L2-dsRNA/SsMBV1 represents missing amino acid residues corresponding to potyvirus 2 helper-component protease sequence. Residues are colored according to a simple property-based scheme, and the position in the original sequence is indicated in the top or bottom line. (B) Comparison of the three-dimensional models of the papain-like cysteine protease from L2-dsRNA/SsMBV1 and potyvirus 2 helper-component protease (Protein Data Bank code c3rnvA). The three-dimensional structural models generated by Phyre2 are based on an alignment generated by hidden Markov model-hidden Markov model matching.

aged in VLPs without L2-dsRNA/SsMBV1. The yield of particles, however, from transfectants carrying L1-dsRNA but lacking L2-dsRNA was significantly lower than original strain SX466 or transfectants carrying both L1- and L2-dsRNA of SsMBV1 (data not shown).

In addition, a horizontal transmission assay was performed between strain SX466 and 1980R via hyphal contact on one PDA plate (Fig. 8A). Two L-dsRNA segments were transmitted from donor strain SX466 to recipient strain 1980R. Interestingly, newly virus-infected isolates were also placed into two groups based on their dsRNA segment content (Fig. 8B). Isolate 1980RV3, which could grow on PDA containing hygromycin, carried both L1- and L2-dsRNA of SsMBV1, whereas isolate 1980RV2, with resistance to hygromycin, harbored only L1-dsRNA/SsMBV1 and lacked L2-dsRNA/SsMBV1 (Fig. 8B). These results are consistent with those of the transfection assays.

Analysis of SsMBV1 VLP structural proteins in absence or presence of L2-dsRNA. To elucidate VLP structure from two groups of transfectants, the VLPs purified from transfectant A367V2 infected by SsMBV1 and from transfectant A367V4 infected by SsMBV1 but lacking L2-dsRNA/SsMBV1, respectively, were denatured and then subjected to SDS-PAGE analysis. Two major protein bands with approximate sizes of 135 kDa and 80 kDa, which were similar in size to virus proteins extracted from strain SX466, were detected whether L2-dsRNA/SsMBV1 was present or absent (Fig. 7C). However, similar proteins were not detected in preparations from the virus-free Ep-1PNA367 strain under the same protocol conditions for the virus-infected strain (Fig. 7C).

VLP proteins p135 and p80 isolated from A367V2 and A367V4, respectively, were further analyzed using PMF-MS. The results of PMS analysis are shown in detail in Tables S1 to S4 in the supplemental material. p135 and p80 of SsMBV1 VLPs isolated from A367V2 generated a total of 52 and 22 peptide fragments, respectively, of which 77% (40/52) of peptide fragments from p135 matched protein encoded by ORF1 and 23% (12/52) of peptide fragments matched protein encoded by ORF2 on L1-dsRNA/SsMBV1 (see Table S1). Forty-one percent (9/22) of peptide fragments from p80 matched protein encoded by ORF1, whereas 45% (10/22) of peptide fragments matched protein encoded by ORF2 (see Table S2). It is of interest that 14% (3/22) of peptide fragments matched ORFB-encoded protein on the L2-dsRNA. p135 and p80 from SsMBV1 VLPs lacking L2-dsRNA generated a total of 65 and 8 peptide fragments, respectively. The sequences of 47 out of 65 peptide fragments corresponded to ORF1-encoded protein p135, and the sequences of the remaining 18 corresponded to

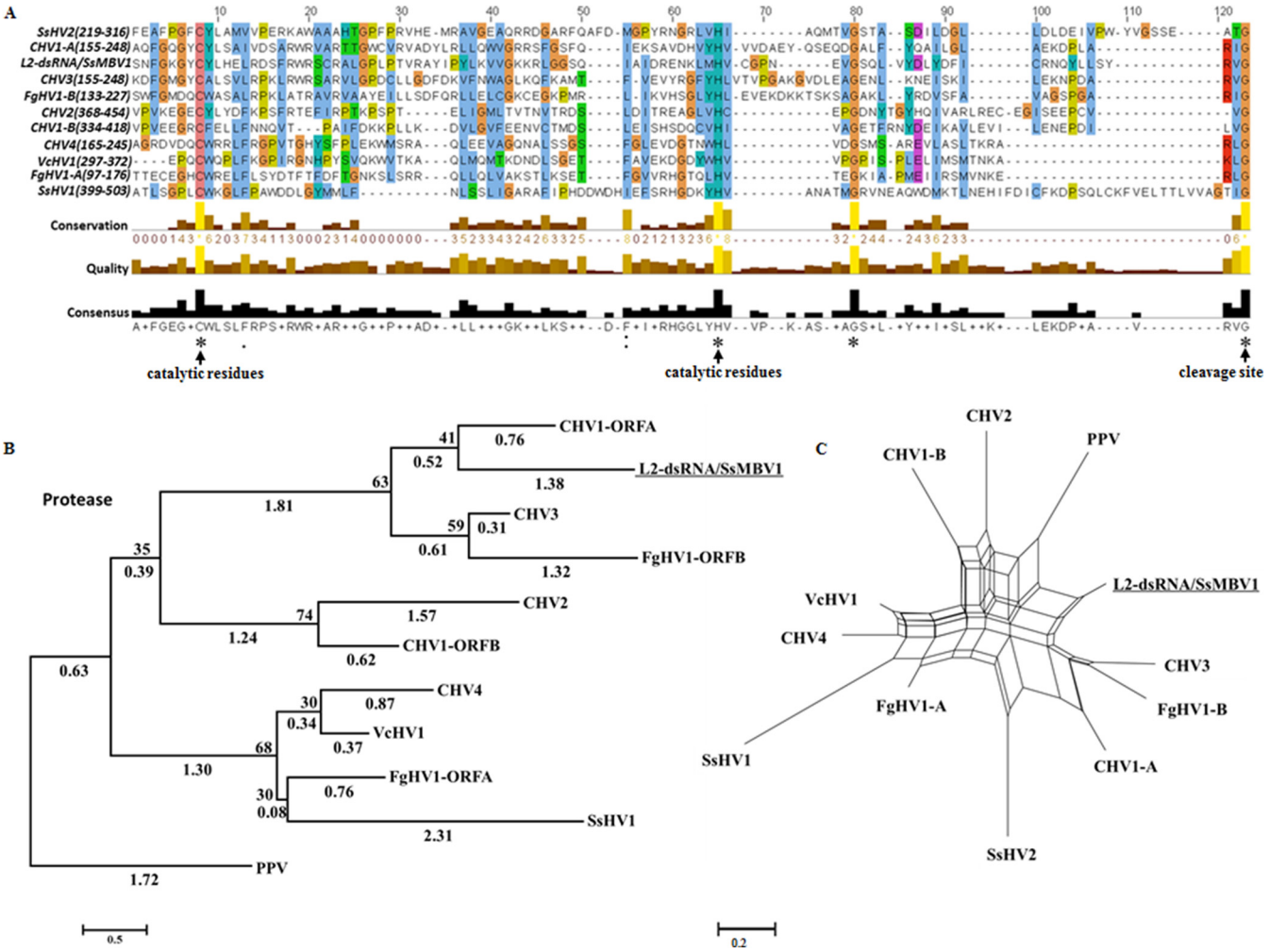

FIG 6 Multiple alignment and phylogenetic analysis of papain-like cysteine protease domain homologs from L2-dsRNA/SsMBV1 and hypoviruses. (A) Multiple alignment of the papain-like cysteine protease in L2-dsRNA/SsMBV1 and several hypoviruses. The default color scheme for ClustalW alignment in the Jalview program was used. Conservation, quality, and consensus are the conservation, quality, and consensus level for multiple alignments, respectively. Identical residues are indicated by asterisks; conserved and semiconserved amino acid residues are indicated by colons and dots, respectively. Catalytic residues and the cleavage site are shown with black arrows. (B) Phylogenetic analysis of L2-dsRNA/SsMBV1 and hypoviruses based on an NJ tree inferred from papain-like cysteine protease domain sequence. The bootstrap values (percent) obtained with 1,000 replicates are indicated on the branches, and branch lengths correspond to the genetic distances under branch lines. The scale bar corresponds to 0.5 amino acid substitutions per site. (C) Neighbor-Net analysis of the papain-like cysteine protease domain homologs. The analysis was conducted under the WAG model of substitution. The scale bar corresponds to 0.2 amino acid substitutions per site. Viruses (abbreviation, strain, GenBank accession number) include *Cryphonectria* hypovirus 1 (CHV1, EP713, NP_041091.1), *Cryphonectria* hypovirus 2 (CHV2, NB58, NP_613266.1), *Cryphonectria* hypovirus 3 (CHV3, GH2, NP_051710.1), *Cryphonectria* hypovirus 4 (CHV4, SR2, YP_138519.1), *Cryphonectria* hypovirus 1 ORFA (CHV1-A, EP713, NP_041090), *Cryphonectria* hypovirus 1 ORFB (CHV1-B, EP713, NP_041091), *Sclerotinia sclerotiorum* hypovirus 1 (SsHV1, SZ-150, AEL99352.1), *Sclerotinia sclerotiorum* hypovirus 2 (SsHV2, SX247, AIA61616.1), *Fusarium graminearum* hypovirus 1 (FgHV1, HN10, AAT07067.2), *Valsa ceratosperma* hypovirus 1 (VcHV1, MVC86, BAM08994.1), *Phomopsis longicolla* hypovirus 1 (PlHV1, ME711, KF537784), and *Fusarium graminearum* virus 1 (FgV1, DK21, AAT07067.2). Plum pox virus (PPV, NP_040807) was used as an outgroup.

ORF2-encoded proteins (28%, 18/65) (see Table S3). On the other hand, p80-derived peptide fragments contained only ORF2-encoded protein sequence (see Table S4). Based on PMF analysis and predicted molecular masses of ORF1- and ORF2-encoded proteins (137 and 126 kDa, respectively), p135 is a mixture of ORF1- and ORF2-encoded proteins. p80 might be generated via different events in processing ORF1- or ORF2-encoded proteins or derived from these two proteins via posttranslational modification.

Taking together the results of genomic sequence analysis of the two dsRNA segments, we presume that SsMBV1 is a novel megabirnavirus with a bisegmented dsRNA genome infecting *S. sclerotiorum*. The definitive nature of L2-dsRNA/SsMBV1, however, is uncertain (whether a genuine genomic virus component or a large satellite-like dsRNA; see Discussion below) and will probably remain so until a naturally occurring nonsegmented "megabirnavirus" is isolated and characterized.

SsMBV1 has slight impact on the biological properties of *S. sclerotiorum*. All mycovirus-free and SsMBV1-infected strains used in the present study were assessed for biological traits, such as colony morphology, growth rate, and virulence. All new mycovirus-infected isolates obtained by two experimental methods of PEG-mediated VLP transfection and horizontal transmission did

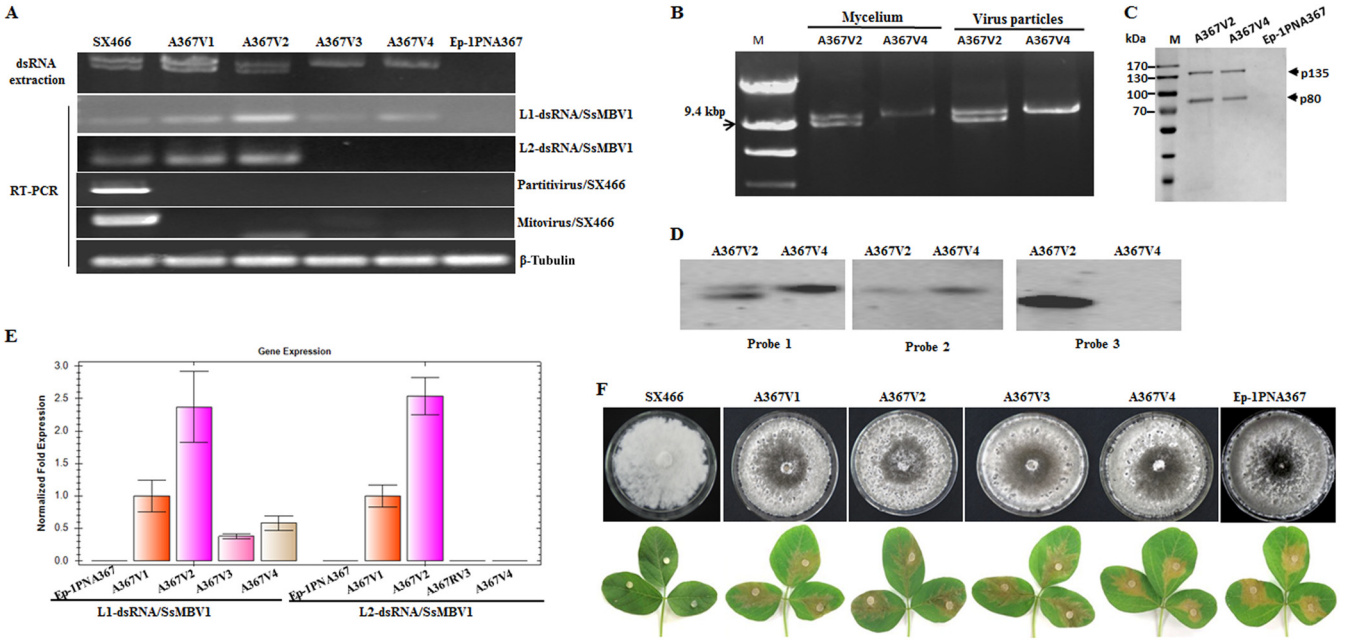

FIG 7 Transfection of protoplasts from virulent strain Ep-1PNA367 of *S. sclerotiorum* with purified SsMBV1 VLPs. (A) Detection of mycoviruses SsMBV1/SX466, mitovirus/SX466, and partitivirus/SX466 in individual isolates using agarose gel electrophoresis of extracted dsRNA and RT-PCR analysis. The β-tubulin gene was used as an internal control. (B) Agarose gel electrophoresis of dsRNA extracted from mycelia of strains A367V2 and A367V4 and VLPs isolated from strains A367V2 and A367V4. (C) SDS-PAGE analysis on a 10% polyacrylamide gel of purified VLPs isolated from strains A367V2 and A367V4 showing two prominent bands. (D) Northern blot detection of dsRNA segments in strains A367V2 and A367V4. The positions of the three probes in dsRNA segments are shown in Fig. 3. (E) Relative transcript accumulation patterns of L1-dsRNA/SsMBV1 and L2-dsRNA/SsMBV1 were assessed by quantitative reverse transcription-PCR amplification in individual transfectants. Total cDNA abundance in the samples was normalized using the tubulin gene as an endogenous reference. Bars indicate standard errors (three replications). (F) Comparison of colony morphologies of parental strains Ep-1PNA367 and SX466 and the virus-transfected isolates A367V1, A367V2, A367V3, and A367V4 on PDA medium (20°C) (upper panels). Virulence assay of parental strains Ep-1PNA367 and SX466 and the virus-transfected isolates A367V1, A367V2, A367V3, and A367V4 (lower panels).

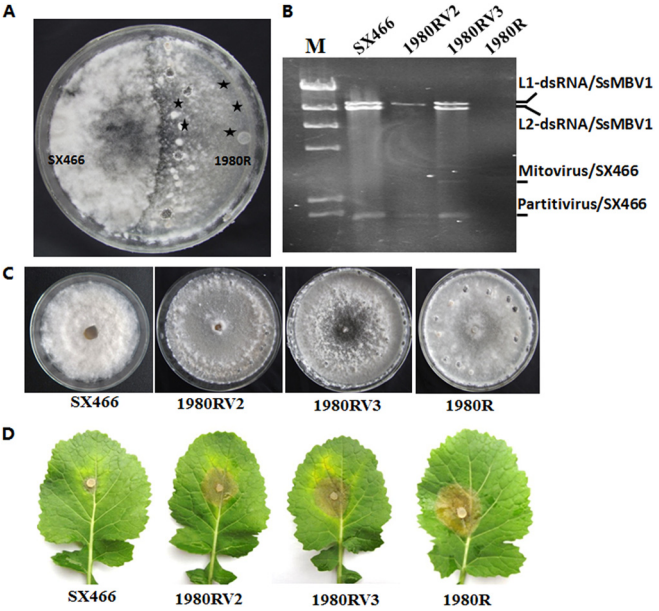

FIG 8 Horizontal transmission of viruses from strain SX466 to virus-free strain 1980R. (A) Strain SX466 was dual cultured with strain 1980R; stars represent the regions where mycelial plugs were cut and then cultured on new PDA containing hygromycin. (B) Agarose gel electrophoresis of dsRNA extracted from mycelia of strains SX466, 1980RV2, 1980RV3, and 1980R. (C) Comparison of colony morphologies of parental strains SX466 and 1980R and newly virus-infected isolates 1980RV2 and 1980RV3 on PDA medium (20°C). (D) Virulence assay of strains on detached leaves of rapeseed.

not show any significant differences from their original virus-free strains (Fig. 7F), which was consistent with the results of virus horizontal transmission (Fig. 8C and D). These results suggested that SsMBV1 has slight or no impact on the biological properties of its hosts, regardless of the presence or absence of L2-dsRNA/SsMBV1. Whether hypovirulence traits of strain SX466 are caused by other mycoviruses or by other biological factors need to be further explored.

DISCUSSION

The fungus *S. sclerotiorum* presents the greatest pathological threat to rapeseed and hosts a multitude of mycoviruses, including dsRNA, ssRNA, and single-stranded DNA (ssDNA) viruses (2, 17). Screening and characterizing more novel mycoviruses will enhance our knowledge of mycovirus diversity in the population of *S. sclerotiorum* and provide new clues for mycovirus evolution and classification. In the present study, the full-length nucleotide sequence of a novel dsRNA mycovirus, SsMBV1, infecting a seemingly hypovirulent strain (SX466) of *S. sclerotiorum*, was determined and its genome organization was characterized.

The present study revealed that SsMBV1 has highest similarity (44% identity) with the previously reported megabirnavirus RnMBV1 based on conserved domains of putative RdRp protein and clustered into an independent phylogenetic clade with four mycoviruses, RnMBV1, PgLV-1, LeMV, and LeSV. The genomes of the three mycoviruses PgLV-1, LeMV, and LeSV comprise one large segment that encodes two putative proteins, but those vi-

ruses appear to be capsidless based on previous reports (38, 39, 40). The RnMBV1 genome was previously reported to comprise two dsRNA segments (dsRNA1 and dsRNA2) (5). RnMBV1-dsRNA2, however, was recently found to be dispensable for replication and encapsidation of RnMBV1. Moreover, RnMBV1-dsRNA1 is still packaged in normal VLPs, and VLP stability and infectivity in its fungal host remain unchanged even when lacking RnMBV1-dsRNA2 (41). Therefore, the phylogenetic clade of SsMBV1 and its phylogenetically related unassigned mycoviruses that have similar genome organizations possibly belong to the family *Megabirnaviridae*, which is distinct from other established ones. However, SsMBV1 is markedly different from RnMVB1 in two aspects: one is that L2-dsRNA of SsMBV1 contains a conserved papain-like protease domain, whereas the dsRNA2 of RnMBV1 lacks such a domain. Another is that SsMBV1 VLPs have two major proteins with molecular masses of 135 kDa and 80 kDa, but RnMBV1 VLPs have a single major protein (135 kDa) and a minor protein with a molecular mass of 250 kDa (5).

Based on sequence analysis and biological data presented in this study, we propose that SsMBV1 might be a novel dsRNA megabirnavirus, although a definitive definition of L2-dsRNA/SsMBV1 (L2-dsRNA) as an authentic genome segment of SsMBV1 (or alternatively as a large satellite-like dsRNA of SsMBV1) remains in dispute. Several lines of evidence have been presented in support of the idea that L2-dsRNA/SsMBV1 might be a satellite-like RNA. First, the L2-dsRNA/SsMBV1 so far has not been found alone by screening all derivatives of strain SX466 but was always associated with the L1-dsRNA/SsMBV1. Second, sequence analysis indicated that L2-dsRNA/SsMBV1 does not encode its own replicase or any conserved replication domains. Therefore, replication of L2-dsRNA/SsMBV1 probably depends on the putative RdRp protein encoded by SsMBV1, and this suggests that L1-dsRNA/SsMBV1 and L2-dsRNA/SsMBV1 are not derived from two independent viruses. Third, SsMBV1 could be encapsidated into viral particles of ~45 nm in diameter. However, SsMBV1 could still be packaged in similar viral particles even in the absence of L2-dsRNA/SsMBV1. Thus, L2-dsRNA/SsMBV1 is not necessary for VLP assembly of SsMBV1. Fourth, when purified VLPs of SsMBV1 from strain SX466 were introduced into protoplasts of virulent strain Ep-1PNA367, two-thirds of newly transfected isolates harbored only L1-dsRNA/SsMBV1 but lacked the L2-dsRNA/SsMBV1, meaning that L2-dsRNA/SsMBV1 could escape from VLPs of SsMBV1 during the SsMBV1 infection process. Based on the combined properties of L2-dsRNA/SsMBV1 and the definition of satellite-like RNAs that rely on helper virus to supply proteins for replication (42, 43), the L2-dsRNA/SsMBV1 could be regarded as a satellite-like RNA of the cognate helper virus SsMBV1.

Several lines of evidence also support the conclusion that the L2-dsRNA/SsMBV1 is a potential genome segment of SsMBV1 based on our present research and previous reports. First, although the second dsRNA segment of SsMBV1 could be lost from new fully viable transfectants, a nonsegmented megabirnavirus has not been detected in natural fungal isolates. Although megabirnavirus genome alterations or rearrangements might happen in newly transfected hosts and thus explain loss of L2-dsRNA, the underlying mechanism remains unknown. Second, VLP protein analysis reveals that the product of L2-dsRNA was detected. Moreover, comparison of different groups of transfectants suggests that L2-dsRNA contributes to a higher transcript level of L1-dsRNA and VLP stability, suggesting that the L2-dsRNA segment helps SsBMV1 to complete the infection cycle in nature. Third, both the 5′ UTRs of the two dsRNA segments (L1- and L2-dsRNA) show extensive conserved sequences (Fig. 3A); this supports the notion that L2-dsRNA/SsMBV1 comprises a genome segment. It is worth mentioning here that conserved terminal sequences between satellites and their helper viruses are believed to be required for recognition by helper virus replicase. Fourth, instances of genome segment alterations are known to occur in mycoviruses as well as in plant viruses. Mycoreovirus 3 (MyRV3) infecting the white root rot fungus contains 12 dsRNA segments in nature, and MyRV3 is able to replicate well after loss of segment S8 during subculturing of infected host fungal strains (44). However, MyRV3 is still considered a mycoreovirus with a 12-segment genome (45). Field isolates of beet necrotic yellow vein virus (BNYVV), a multipartite +ssRNA virus, usually consist of five RNA components, whereas only the two or three largest segments are responsible for systemic infection of host plants in the laboratory (46, 47, 48). However, researchers still describe the BNYVV genome as consisting of five segments.

Interestingly, a conserved papain-like protease domain, phylogenetically related to protease p29 of CHV1-ORFA, was discovered in ORFA-encoded protein of L2-dsRNA/SsMBV1. This protease domain commonly occurs in ssRNA viruses, including members of families *Potyviridae* and *Hypoviridae*, but not in dsRNA viruses. The protease domain of hypoviruses has been shown to be responsible for autoproteolytic processing events, and polyprotein p69 was autocatalytically cleaved into two mature products, p29 and p40, by a papain-like protease domain within p29 in CHV1-ORFA (49). Protease p29 has been confirmed to be a multifunctional protein of major significance for viral replication and RNA accumulation in the host. These effects are now generally ascribed to the role of suppression of the RNA silencing antiviral defense response (50, 51, 52, 53). Whether the papain-like protease in SsMBV1 has functions similar to CHV1 p29 needs to be further explored.

The events of horizontal gene transfer (HGT) commonly occur not only between distinct evolutionary lineages of ssRNA, dsRNA, or DNA viruses but also between DNA and ssRNA viruses (7, 54, 55, 56, 57, 58, 59, 60). These HGT events have been a major contributor of evolutionary innovation and a driver of speciation and environmental adaptation for viruses. However, no example of HGT has been reported between dsRNA and ssRNA viruses. In the present study, an interesting feature is that a papain-like protease domain (Peptidase_C7 superfamily) is shared between a dsRNA virus (L2-dsRNA/SsMBV1) and an ssRNA hypovirus of the family *Hypoviridae*. Our study provides three lines of evidence that support the conclusion that HGT occurred between L2-dsRNA/SsMBV1 and a hypovirus. First, L2-dsRNA/SsMBV1 does contain a conserved domain of the papain-like protease based on sequence analysis, and a similar protease commonly exists in all known hypoviruses but is missing in dsRNA viruses. Second, phylogenetic analysis suggests that L2-dsRNA/SsMBV1-encoded protease is phylogenetically related to those encoded by hypoviruses CHV1, CHV3, and FgHV1 and formed an independent clade that is distantly related to other hypoviruses. Third, the conserved protease domain, phylogenetically related to CHV-1 p29, is situated at the N-terminal portion of the ORFA-encoded protein of L2-dsRNA/SsMBV1, but the sequence derived from the C-terminal portion of the ORFA-encoded protein has high sequence identity

to the corresponding region of the C terminus of the ORF3-encoded protein of dsRNA2/RnMBV1. This phenomenon thus reveals that the ORFA-encoded protein of L2-dsRNA/SsMBV1 is produced as a consequence of recombinational events between different viruses. Moreover, several *S. sclerotiorum* isolates have been confirmed to be infected with hypoviruses (23, 61, 62, 63), suggesting that some hosts provided opportunities for HGT between hypovirus and SsMBV1 during evolutionary processes. Based on the data presented here, we hypothesize that HGT might have occurred from a hypovirus to a dsRNA genomic component of SsMBV1 (or alternatively to an unusually large satellite-like dsRNA dependent on SsMBV1 for replication and encapsidation). This finding provides new insights into the evolutionary history of dsRNA and ssRNA viruses.

ACKNOWLEDGMENTS

This research was supported by China National Funds for Distinguished Young Scientists (31125023), the Special Fund for Agro-scientific Research in the Public Interest (201103016), and the Key Project of the Chinese Ministry of Education (313024). The funding agencies had no role in study design, data collection and analysis, decision to publish, or preparation of the manuscript.

We also thank the anonymous reviewers for their valuable comments.

REFERENCES

1. **Ghabrial SA, Suzuki N.** 2009. Viruses of plant pathogenic fungi. Annu Rev Phytopathol **47:**353–384. http://dx.doi.org/10.1146/annurev-phyto-080508-081932.
2. **Xie J, Jiang D.** 2014. New insights into mycoviruses and exploration for the biological control of crop fungal diseases. Annu Rev Phytopathol **52:**45–68. http://dx.doi.org/10.1146/annurev-phyto-102313-050222.
3. **Liu L, Xie J, Cheng J, Fu Y, Li G, Yi X, Jiang D.** 2014. Fungal negative-stranded RNA virus that is related to bornaviruses and nyaviruses. Proc Natl Acad Sci U S A **111:**12205–12210. http://dx.doi.org/10.1073/pnas.1401786111.
4. **Ghabrial SA, Castón JR, Jiang D, Nibert ML, Suzuki N.** 2015. 50-plus years of fungal viruses. Virology **479-480C:**356–368. http://dx.doi.org/10.1016/j.virol.2015.02.034.
5. **Chiba S, Salaipeth L, Lin Y, Sasaki A, Kanematsu S, Suzuki N.** 2009. A novel bipartite double-stranded RNA mycovirus from the white root rot fungus *Rosellinia necatrix*: molecular and biological characterization, taxonomic considerations, and potential for biological control. J Virol **83:**12801–12812. http://dx.doi.org/10.1128/JVI.01830-09.
6. **Lin YH, Chiba S, Tani A, Kondo H, Sasaki A, Kanematsu S, Suzuki N.** 2012. A novel quadripartite dsRNA virus isolated from a phytopathogenic filamentous fungus, *Rosellinia necatrix*. Virology **426:**42–50. http://dx.doi.org/10.1016/j.virol.2012.01.013.
7. **Liu H, Fu Y, Xie J, Cheng J, Ghabrial SA, Li G, Yi X, Jiang D.** 2012. Evolutionary genomics of mycovirus-related dsRNA viruses reveals cross-family horizontal gene transfer and evolution of diverse viral lineages. BMC Evol Biol **12:**91. http://dx.doi.org/10.1186/1471-2148-12-91.
8. **Wu M, Jin F, Zhang J, Yang L, Jiang D, Li G.** 2012. Characterization of a novel bipartite double-stranded RNA mycovirus conferring hypovirulence in the phytopathogenic fungus *Botrytis porri*. J Virol **86:**6605–6619. http://dx.doi.org/10.1128/JVI.00292-12.
9. **Jian J, Lakshman DK, Tavantzis SM.** 1997. Association of distinct double-stranded RNAs with enhanced or diminished virulence in *Rhizoctonia solani* infecting potato. Mol Plant Microbe Interact **10:**1002–1009. http://dx.doi.org/10.1094/MPMI.1997.10.8.1002.
10. **Márquez LM, Redman RS, Rodriguez RJ, Roossinck MJ.** 2007. A virus in a fungus in a plant: three-way symbiosis required for thermal tolerance. Science **315:**513–515. http://dx.doi.org/10.1126/science.1136237.
11. **Pearson MN, Beever RE, Boine B, Arthur K.** 2009. Mycoviruses of filamentous fungi and their relevance to plant pathology. Mol Plant Pathol **10:**115–128. http://dx.doi.org/10.1111/j.1364-3703.2008.00503.x.
12. **Anagnostakis SL.** 1982. Biological control of chestnut blight. Science **215:**466–471. http://dx.doi.org/10.1126/science.215.4532.466.
13. **Nuss DL.** 2005. Hypovirulence: mycoviruses at the fungal-plant interface. Nat Rev Microbiol **3:**632–642. http://dx.doi.org/10.1038/nrmicro1206.
14. **Yu X, Li B, Fu Y, Jiang D, Ghabrial SA, Li G, Peng Y, Xie J, Cheng J, Huang J, Yi X.** 2010. A geminivirus-related DNA mycovirus that confers hypovirulence to a plant pathogenic fungus. Proc Natl Acad Sci U S A **107:**8387–8392. http://dx.doi.org/10.1073/pnas.0913535107.
15. **Yu X, Li B, Fu Y, Xie J, Cheng J, Ghabrial SA, Li G, Yi X, Jiang D.** 2013. Extracellular transmission of a DNA mycovirus and its use as a natural fungicide. Proc Natl Acad Sci U S A **110:**1452–1457. http://dx.doi.org/10.1073/pnas.1213755110.
16. **Bolton MD, Thomma BPHJ, Nelson BD.** 2006. *Sclerotinia sclerotiorum* (Lib.) de Bary: biology and molecular traits of a cosmopolitan pathogen. Mol Plant Pathol **7:**1–16. http://dx.doi.org/10.1111/j.1364-3703.2005.00316.x.
17. **Jiang D, Fu Y, Li G, Ghabrial SA.** 2013. Viruses of the plant pathogenic fungus *Sclerotinia sclerotiorum*. Adv Virus Res **86:**215–248. http://dx.doi.org/10.1016/B978-0-12-394315-6.00008-8.
18. **Xu Z, Wu S, Liu L, Cheng J, Fu Y, Jiang D, Xie J.** 2015. A mitovirus related to plant mitochondrial gene confers hypovirulence on the phytopathogenic fungus *Sclerotinia sclerotiorum*. Virus Res **197:**127–136. http://dx.doi.org/10.1016/j.virusres.2014.12.023.
19. **Xie J, Wei D, Jiang D, Fu Li YG, Ghabrial SA, Peng Y.** 2006. Characterization of debilitation-associated mycovirus infecting the plant-pathogenic fungus *Sclerotinia sclerotiorum*. J Gen Virol **87:**241–249. http://dx.doi.org/10.1099/vir.0.81522-0.
20. **Amselem J, Cuomo CA, van Kan JA, Viaud M, Benito EP, Couloux A, Coutinho PM, de Vries RP, Dyer PS, Fillinger S, Fournier E, Gout L, Hahn M, Kohn L, Lapalu N, Plummer KM, Pradier JM, Quevillon E, Sharon A, Simon A, ten Have A, Tudzynski B, Tudzynski P, Wincker P, Andrew M, Anthouard V, Beever RE, Beffa R, Benoit I, Bouzid O, Brault B, Chen Z, Choquer M, Collemare J, Cotton P, Danchin EG, Da Silva C, Gautier A, Giraud C, Giraud T, Gonzalez C, Grossetete S, Guldener U, Henrissat B, Howlett BJ, Kodira C, Kretschmer M, Lappartient A, Leroch M, Levis C, Mauceli E, Neuveglise C, Oeser B, Pearson M, Poulain J, Poussereau N, Quesneville H, Rascle C, Schumacher J, Segurens B, Sexton A, Silva E, Sirven C, Soanes DM, Talbot NJ, Templeton M, Yandava C, Yarden O, Zeng Q, Rollins JA, Lebrun MH, Dickman M.** 2011. Genomic analysis of the necrotrophic fungal pathogens *Sclerotinia sclerotiorum* and *Botrytis cinerea*. PLoS Genet **7:**e1002230. http://dx.doi.org/10.1371/journal.pgen.1002230.
21. **Xiao X, Cheng J, Tang J, Fu Y, Jiang D, Baker TS, Ghabrial SA, Xie J.** 2014. A novel partitivirus that confers hypovirulence on plant pathogenic fungi. J Virol **88:**10120–10133. http://dx.doi.org/10.1128/JVI.01036-14.
22. **Jiang D, Ghabrial SA.** 2004. Molecular characterization of Penicillium chrysogenum virus: reconsideration of the taxonomy of the genus *Chrysovirus*. J Gen Virol **85:**2111–2121. http://dx.doi.org/10.1099/vir.0.79842-0.
23. **Xie J, Xiao X, Fu Y, Liu H, Cheng J, Ghabrial SA, Li G, Jiang D.** 2011. A novel mycovirus closely related to hypoviruses that infects the plant pathogenic fungus Sclerotinia sclerotiorum. Virology **418:**49–56. http://dx.doi.org/10.1016/j.virol.2011.07.008.
24. **Potgieter AC, Page NA, Liebenberg J, Wright IM, Land O, van Dijk AA.** 2009. Improved strategies for sequence-independent amplification and sequencing of viral double-stranded RNA genomes. J Gen Virol **90:**1423–1432. http://dx.doi.org/10.1099/vir.0.009381-0.
25. **Thompson JD, Gibson TJ, Plewniak F.** 1997. The Clustal X windows interface: flexible strategies for multiple sequence alignment aided by quality analysis tools. Nucleic Acids Res **25:**4876–4882. http://dx.doi.org/10.1093/nar/25.24.4876.
26. **Tamura K, Peterson D, Peterson N, Stecher G, Nei M, Kumar S.** 2011. MEGA5: molecular evolutionary genetics analysis using maximum likelihood, evolutionary distance, and maximum parsimony methods. Mol Biol Evol **28:**2731–2739. http://dx.doi.org/10.1093/molbev/msr121.
27. **Huson DH, Bryant D.** 2006. Application of phylogenetic networks in evolutionary studies. Mol Biol Evol **23:**254–267.
28. **Zuker M.** 2003. Mfold web server for nucleic acid folding and hybridization prediction. Nucleic Acids Res **31:**3406–3415. http://dx.doi.org/10.1093/nar/gkg595.
29. **Sperschneider J, Datta A.** 2010. DotKnot: pseudoknot prediction using the probability dot plot under a refined energy model. Nucleic Acids Res **38:**e103. http://dx.doi.org/10.1093/nar/gkq021.
30. **Kelley LA, Sternberg MJE.** 2009. Protein structure prediction on the web: a case study using the Phyre server. Nat Protoc **4:**363–371. http://dx.doi.org/10.1038/nprot.2009.2.
31. **Zhang L, Fu Y, Xie J, Jiang D, Li G, Yi X.** 2009. A novel virus that

infecting hypovirulent strain XG36-1 of plant fungal pathogen *Sclerotinia sclerotiorum*. Virol J **6:**96. http://dx.doi.org/10.1186/1743-422X-6-96.
32. **Hillman BI, Esteban R.** 2011. Family *Narnaviridae*, p 1055–1060. *In* King AMQ, Adams MJ, Carstens EB, Lefkowitz EJ (ed), Virus taxonomy: classification and nomenclature of viruses. Ninth report of the International Committee on Taxonomy of Viruses. Elsevier Academic Press, London, United Kingdom.
33. **Huang X, Yang Y, Wang G, Cheng Q, Du Z.** 2014. Highly conserved RNA pseudoknots at the Gag-Pol junction of HIV-1 suggest a novel mechanism of −1 ribosomal frameshifting. RNA **20:**587–593. http://dx.doi.org/10.1261/rna.042457.113.
34. **Dinman JD, Icho T, Wickner RB.** 1991. A −1 ribosomal frameshift in a double-stranded RNA virus of yeast forms a gag-pol fusion protein. Proc Natl Acad Sci U S A **88:**174–178. http://dx.doi.org/10.1073/pnas.88.1.174.
35. **Xie P.** 2013. A dynamical model of programmed −1 ribosomal frameshifting. J Theor Biol **336:**119–131. http://dx.doi.org/10.1016/j.jtbi.2013.07.022.
36. **Li H, Havens WM, Nibert ML, Ghabrial SA.** 2011. RNA sequence determinants of a coupled termination-reinitiation strategy for downstream open reading frame translation in *Helminthosporium victoriae virus* 190S and other victoriviruses (family *Totiviridae*). J Virol **85:**7343–7352. http://dx.doi.org/10.1128/JVI.00364-11.
37. **Valli A, Gallo A, Calvo M, de Jesús Pérez J, García JA.** 2014. A novel role of the potyviral helper component proteinase contributes to enhance the yield of viral particles. J Virol **88:**9808–9818. http://dx.doi.org/10.1128/JVI.01010-14.
38. **Kozlakidis Z, Hacker CV, Bradley D, Jamal A, Phoon X, Webber J, Brasier CM, Buck KW, Coutts RHA.** 2009. Molecular characterization of two novel double-stranded RNA elements from *Phlebiopsis gigantea*. Virus Genes **39:**132–136. http://dx.doi.org/10.1007/s11262-009-0364-z.
39. **Lim JM, Jamal A, Phoon X, Korhonen K, Coutts RH.** 2011. Incidence of Phlebiopsis gigantea large virus-1 in a collection of *Phlebiopsis gigantea* isolates. Arch Virol **156:**2091–2094. http://dx.doi.org/10.1007/s00705-011-1086-9.
40. **Won HK, Park SJ, Kim DK, Shin MJ, Kim N, Lee SH, Kwon YC, Ko HK, Ro HS, Lee HS.** 2013. Isolation and characterization of a mycovirus in *Lentinula edodes*. J Microbiol **51:**118–122. http://dx.doi.org/10.1007/s12275-013-2351-2.
41. **Kanematsu S, Shimizu T, Salaipeth L, Yaegashi H, Sasaki A, Ito T, Suzuki N.** 2014. Genome rearrangement of a mycovirus Rosellinia necatrix megabirnavirus 1 affecting its ability to attenuate virulence of the host fungus. Virology **450-451:**308–315. http://dx.doi.org/10.1016/j.virol.2013.12.002.
42. **Bruening G.** 2001. Virus-dependent RNA agents, p 1170–1177. *In* Maloy O, Murray T (ed), Encyclopedia of plant pathology, vol 2. John Wiley & Sons, New York, NY.
43. **Briddon RW, Ghabrial SA, Lin NS, Palukaitis P, Scholthof KBG, Vetten HJ.** 2011. Satellites and other virus-dependent nucleic acids, p 1211–1219. *In* King AMQ, Adams MJ, Carstens EB, Lefkowitz EJ (ed), Virus taxonomy: classification and nomenclature of viruses. Ninth report of the International Committee on Taxonomy of Viruses. Elsevier Academic Press, London, United Kingdom.
44. **Tanaka T, Eusebio-Cope A, Sun L, Suzuki N.** 2012. Mycoreovirus genome alterations: similarities to and differences from rearrangements reported for other reoviruses. Front Microbiol **3:**186. http://dx.doi.org/10.3389/fmicb.2012.00186.
45. **Attoui H, Mertens PPC, Becnel J, Belaganahalli S, Bergoin M, Brussaard CP, Chappell JD, Ciarlet M, del Vas M, Dermody TS, Dormitzer PR, Duncan R, Fcang Q, Graham R, Guglielmi KM, Harding RM, Hillman B, Makkay A, Marzachì C, Matthijnssens J, Milne RG, Mohd Jaafar F, Mori H, Noordeloos AA, Omura T, Patton JT, Rao S, Maan M, Stoltz D, Suzuki N, Upadhyaya NM, Wei C, Zhou H.** 2011. Family *Reoviridae*, p 541–637. *In* King AMQ, Adams MJ, Carstens EB, Lefkowitz EJ (ed), Virus taxonomy: classification and nomenclature of viruses. Ninth report of the International Committee on Taxonomy of Viruses. Elsevier Academic Press, London, United Kingdom.
46. **Peltier C, Klein E, Hleibieh K, D'Alonzo M, Hammann P, Bouzoubaa S, Ratti C, Gilmer D.** 2012. Beet necrotic yellow vein virus subgenomic RNA3 is a cleavage product leading to stable non-coding RNA required for long-distance movement. J Gen Virol **93:**1093–1102. http://dx.doi.org/10.1099/vir.0.039685-0.
47. **Chiba S, Kondo H, Miyanishi M, Andika IB, Han C, Tamada T.** 2011. The evolutionary history of beet necrotic yellow vein virus deduced from genetic variation, geographical origin and spread, and the breaking of host resistance. Mol Plant Microbe Interact **24:**207–218. http://dx.doi.org/10.1094/MPMI-10-10-0241.
48. **Gilmer D, Ratti C.** 2011. Genus *Benyvirus*, p 1163–1068. *In* King AMQ, Adams MJ, Carstens EB, Lefkowitz EJ (ed), Virus taxonomy: classification and nomenclature of viruses. Ninth report of the International Committee on Taxonomy of Viruses. Elsevier Academic Press, London, United Kingdom.
49. **Choi GH, Pawlyk DM, Nuss DL.** 1991. The autocatalytic protease p29 encoded by a hypovirulence-associated virus of the chestnut blight fungus resembles the potyvirus-encoded protease HC-Pro. Virology **183:**747–752. http://dx.doi.org/10.1016/0042-6822(91)91004-Z.
50. **Segers GC, Zhang X, Deng F, Sun Q, Nuss DL.** 2007. Evidence that RNA silencing functions as an antiviral defense mechanism in fungi. Proc Natl Acad Sci U S A **104:**12902–12906. http://dx.doi.org/10.1073/pnas.0702500104.
51. **Suzuki N, Maruyama K, Moriyama M, Nuss DL.** 2003. Hypovirus papain-like protease p29 functions in trans to enhance viral double-stranded RNA accumulation and vertical transmission. J Virol **77:**11697–11707. http://dx.doi.org/10.1128/JVI.77.21.11697-11707.2003.
52. **Sun Q, Choi GH, Nuss DL.** 2009. A single *Argonaute* gene is required for induction of RNA silencing antiviral defense and promotes viral RNA recombination. Proc Natl Acad Sci U S A **106:**17927–17932. http://dx.doi.org/10.1073/pnas.0907552106.
53. **Jensen KS, Nuss DL.** 2014. Mutagenesis of the catalytic and cleavage site residues of the hypovirus papain-like proteases p29 and p48 reveals alternative processing and contributions to optimal viral RNA accumulation. J Virol **88:**11946–11954. http://dx.doi.org/10.1128/JVI.01489-14.
54. **La Scola B, Desnues C, Pagnier I, Robert C, Barrassi L, Fournous G, Merchat M, Suzan-Monti M, Forterre P, Koonin E, Raoult D.** 2008. The virophage as a unique parasite of the giant mimivirus. Nature **455:**100–104. http://dx.doi.org/10.1038/nature07218.
55. **Diemer GS, Stedman KM.** 2012. A novel virus genome discovered in an extreme environment suggests recombination between unrelated groups of RNA and DNA viruses. Biol Direct **7:**13. http://dx.doi.org/10.1186/1745-6150-7-13.
56. **Koonin EV, Dolja VV.** 2012. Expanding networks of RNA virus evolution. BMC Biol **10:**54. http://dx.doi.org/10.1186/1741-7007-10-54.
57. **Lang AS, Zhaxybayeva O, Beatty JT.** 2012. Gene transfer agents: phage-like elements of genetic exchange. Nat Rev Microbiol **10:**472–482. http://dx.doi.org/10.1038/nrmicro2802.
58. **Krupovic M.** 2013. Networks of evolutionary interactions underlying the polyphyletic origin of ssDNA viruses. Curr Opin Virol **3:**578–586. http://dx.doi.org/10.1016/j.coviro.2013.06.010.
59. **Qin XC, Shi M, Tian JH, Lin XD, Gao DY, He JR, Wang JB, Li CX, Kang YJ, Yu B, Zhou DJ, Xu J, Plyusnin A, Holmes EC, Zhang YZ.** 2014. A tick-borne segmented RNA virus contains genome segments derived from unsegmented viral ancestors. Proc Natl Acad Sci U S A **111:**6744–6749. http://dx.doi.org/10.1073/pnas.1324194111.
60. **Krupovic M, Koonin EV.** 2014. Evolution of eukaryotic single-stranded DNA viruses of the *Bidnaviridae* family from genes of four other groups of widely different viruses. Sci Rep **4:**5347. http://dx.doi.org/10.1038/srep05347.
61. **Hu Z, Wu S, Cheng J, Fu Y, Jiang D, Xie J.** 2014. Molecular characterization of two positive-strand RNA viruses co-infecting a hypovirulent strain of *Sclerotinia sclerotiorum*. Virology **464-465:**450–459. http://dx.doi.org/10.1016/j.virol.2014.07.007.
62. **Khalifa ME, Pearson MN.** 2014. Characterisation of a novel hypovirus from *Sclerotinia sclerotiorum* potentially representing a new genus within the *Hypoviridae*. Virology **464-465:**441–449. http://dx.doi.org/10.1016/j.virol.2014.07.005.
63. **Marzano SY, Hobbs HA, Nelson BD, Hartman GL, Eastburn DM, McCoppin NK, Domier LL.** 2015. Transfection of *Sclerotinia sclerotiorum* with in vitro transcripts of a naturally occurring interspecific recombinant of Sclerotinia sclerotiorum hypovirus 2 significantly reduces virulence of the fungus. J Virol **89:**5060–5071. http://dx.doi.org/10.1128/JVI.03199-14.